Published OnlineFirst June 21, 2019; DOI: 10.1158/1535-7163.MCT-18-0624

Large Molecule Therapeutics

Molecular Cancer Therapeutics

MEN1309/OBT076, a First-In-Class Antibody–Drug Conjugate Targeting CD205 in Solid Tumors

Giuseppe Merlino[1], Alessio Fiascarelli[1], Mario Bigioni[1], Alessandro Bressan[1], Corrado Carrisi[1], Daniela Bellarosa[1], Massimiliano Salerno[1], Rossana Bugianesi[2], Rosanna Manno[3], Cristina Bernadó Morales[4], Joaquin Arribas[4,5,6], Rachel L. Dusek[7], James E. Ackroyd[7], Phuoc Huy Pham[7], Rahel Awdew[7], Dee Aud[7], Michael Trang[7], Carmel M. Lynch[7], Jonathan Terrett[7], Keith E. Wilson[7], Christian Rohlff[7], Stefano Manzini[8], Andrea Pellacani[8], and Monica Binaschi[1]

Abstract

CD205 is a type I transmembrane glycoprotein and is a member of the C-type lectin receptor family. Analysis by mass spectrometry revealed that CD205 was robustly expressed and highly prevalent in a variety of solid malignancies from different histotypes. IHC confirmed the increased expression of CD205 in pancreatic, bladder, and triple-negative breast cancer (TNBC) compared with that in the corresponding normal tissues. Using immunofluorescence microscopy, rapid internalization of the CD205 antigen was observed. These results supported the development of MEN1309/OBT076, a fully humanized CD205-targeting mAb conjugated to DM4, a potent maytansinoid derivate, via a cleavable N-succinimidyl-4-(2-pyridyldithio) butanoate linker. MEN1309/OBT076 was characterized *in vitro* for target binding affinity, mechanism of action, and cytotoxic activity against a panel of cancer cell lines. MEN1309/OBT076 displayed selective and potent cytotoxic effects against tumor cells exhibiting strong and low to moderate CD205 expression. *In vivo*, MEN1309/OBT076 showed potent antitumor activity resulting in durable responses and complete tumor regressions in many TNBC, pancreatic, and bladder cancer cell line–derived and patient-derived xenograft models, independent of antigen expression levels. Finally, the pharmacokinetics and pharmacodynamic profile of MEN1309/OBT076 was characterized in pancreatic tumor–bearing mice, demonstrating that the serum level of antibody–drug conjugate (ADC) achieved through dosing was consistent with the kinetics of its antitumor activity. Overall, our data demonstrate that MEN1309/OBT076 is a novel and selective ADC with potent activity against CD205-positive tumors. These data supported the clinical development of MEN1309/OBT076, and further evaluation of this ADC is currently ongoing in the first-in-human SHUTTLE clinical trial.

Introduction

Antibody–drug conjugates (ADC) utilize a novel anticancer approach based on the specificity of mAbs and their ability to deliver a highly potent cytotoxic payload inside target cells (1). These therapeutic agents comprise three components: (i) the antibody, which recognizes a specific tumor-associated antigen, (ii) the chemical linker, designed to release the cytotoxic agent within the cell, and (iii) the payload, usually a low molecular weight molecule that acts as a very potent cytotoxic agent. The combination of these three moieties allows delivery of toxic drugs to cancer cells, while minimizing systemic exposure (2). Indeed, the target specificity and the chemical structure of the linker are accurately designed to render the payload of the ADC inactive while in circulation, but readily cleaved and released, through one of several mechanisms, within the antigen-positive cells (3–4).

[1]Department of Experimental and Translational Oncology, Menarini Ricerche SpA, Pomezia, Rome, Italy. [2]Department of Pharmacokinetics and Metabolism, Menarini Ricerche, Pomezia, Rome, Italy. [3]Research Toxicology Center, Pomezia, Rome, Italy. [4]Preclinical Research Program, Vall D'Hebron, Institute of Oncology and Centro de Investigación Biomédica en Red en Oncologia (CIBERONC), Barcelona, Spain. [5]Department of Biochemistry and Molecular Biology, Universitat Autonoma de Barcelona, Campus de la UAB, Bellaterra, Spain. [6]Institució Catalana de Recerca i Estudis Avançats (ICREA), Barcelona, Spain. [7]Oxford BioTherapeutics, Ltd., Abingdon, United Kingdom. [8]Menarini Ricerche S.p.A - Menarini Group, Florence, Italy.

Note: Supplementary data for this article are available at Molecular Cancer Therapeutics Online (http://mct.aacrjournals.org/).

G. Merlino and A. Fiascarelli contributed equally to this article.

Current address for R.L. Dusek: Clovis Oncology, San Francisco, California; current address for P.H. Pham, University of Wisconsin, Madison, Wisconsin; current address for R. Awdew, Incyte, Leatherhead, United Kingdom; current address for D. Aud, Entrepreneur, Irvine, California; current address for M. Trang, Antibody Solutions, Sunnyvale, California; current address for C.M. Lynch, Lira Biotech Consulting, LLC, Seattle, Washington; current address for J. Terrett, CRISPER, Cambridge, Massachusetts; and current address for K.E. Wilson, NALO Therapeutics, San Francisco, California.

Corresponding Author: Giuseppe Merlino, Menarini Ricerche SpA, Via Tito Speri, 10, Pomezia, Rome 00071, Italy. Phone: 3906-9118-4463; Fax: 3906-9100-220; E-mail: gmerlino@menarini-ricerche.it

Mol Cancer Ther 2019;18:1533–43

doi: 10.1158/1535-7163.MCT-18-0624

Published OnlineFirst June 21, 2019; DOI: 10.1158/1535-7163.MCT-18-0624

Currently there are four ADCs approved for clinical use (5). However, there remains an unmet need for effective therapies in many patient populations. Given the promise of ADCs for precision cancer therapy, the identification of novel targets and development of unique therapeutics is paramount. Using the OGAP target discovery system (6) to incorporate molecular, cellular, phenotypic, and clinical information with protein and gene expression data from a panel of tumor and normal tissues, we identified CD205 as one such target.

CD205 is a type I transmembrane protein that belongs to the macrophage mannose receptor family of C-type lectins (7, 8). The C-type lectin receptors are a large superfamily of multi-functional extracellular proteins containing C-type lectin-like domains (CTLD), double loop structures with Ca^{2+}-dependent carbohydrate binding activity (9). The extracellular domain of the protein consists of a cysteine-rich domain, a fibronectin type II domain, and 10 tandem repeated CTLDs. The short cytoplasmic tail contains motifs for amino acid–based endocytosis (10), consistent with its described role as an endocytic receptor in dendritic and thymic epithelial cells (11). Recently, it has been reported that CD205 plays a role in the immune clearance as a recognition receptor for apoptotic and necrotic cells (12–14). In addition to its physiologic role in the immune system, it was recently demonstrated that CD205 modulates the cellular phenotype and invasiveness of ovarian cancer cells (15, 16).

Our results highlight characteristics of CD205, such as differential cell surface expression in multiple human cancers compared with healthy tissues and a rapid internalization rate that indicates this antigen may be an ideal target for an ADC therapy. Herein, we discuss the activity of a new ADC, MEN1309/OBT076. The molecule consists of a novel anti-CD205 human antibody conjugated through a cleavable N-succinimidyl-4-(2-pyridyldithio) butanoate (SPDB) linker to the microtubule disrupting agent DM4 (17, 18).

Materials and Methods

Antibodies and reagents

MBH1309/OBT076, a fully human mAb which specifically binds to CD205, was produced using the human transgenic Xenomouse Platform (Amgen). Mice were immunized with CHO cells transfected with full length CD205. Approximately 1,400 hybridoma clones were screened for binding specificity to CD205 by flow cytometry on HEK293 cells transfected with full length CD205 and HT29 cells endogenously expressing the target, as well as for cytotoxicity potential when bound to DM1-Fab anti-human IgG in cell viability assays. OBT076_16A5 was selected as lead clone. A CHO-derived cell line was developed using the GS Gene Expression System (Lonza). The variable region sequence for the antibody's heavy and light chain was cloned into the Lonza GS plasmid, which was stably expressed in CHO-K1SV cells. The antibody was produced from this cell line at Menarini Biotech. The antibody was conjugated to DM4 at Piramal, to produce the MEN1309 ADC (19). The average drug:antibody ratio of MEN1309 was approximately 1:3.7.

Cell lines

All cancer cell lines used were purchased from the ATCC and Deutsche Sammlung von Mikroorganismen und Zellkulturen and cultured following the manufacturer's instructions. *Mycoplasma* testing was not performed on *in vitro* propagated cultures, which were maintained for maximal 4 months. No additional authentication method was performed.

Human tissue microarrays, IHC, and visual scoring

Formalin-fixed, paraffin-embedded (FFPE) human tumor tissue microarrays (TMA) or gross tissue sections were used to assess expression of CD205 antigen in multiple solid human cancers along with xenograft tumors. A total of seven commercial tumor TMAs representing seven different solid tumor types were purchased (US Biomax and Tristar) for this evaluation (Supplementary Table S1).

Estimation of antigen per cells by quantitative flow cytometry

Cell surface CD205 antigen expression levels were measured using BD Bioscience Quantibrite Kit. The CD205 antigen density on the selected cancer cell lines was quantified determining the PE-conjugated MEN1309/OBT076 bound per cell. Briefly, special calibrated beads generate a standard curve that converts MFI into fluorochrome molecule number, which in turn corresponds to the number of antigens per cell. Adherent cells were detached using 1× Cell Dissociation Non Enzymatic Solution (Sigma Aldrich) and resuspended in PBS + 0.5% BSA (Miltenyi Biotec). One-hundred microliter of cell solution (3×10^5 cells) were dispensed in 5 mL flow cytometric tubes and 5 μL of FcR Blocking (Miltenyi Biotec) were added. After 10 minutes at 4°C, 10 μL of different dilutions of the PE-conjugated MEN1309/OBT076 (ranging between 0.1 and 20 μg/mL) were added. Acquisition of data was carried out using a FACS Canto II. For each sample, mean fluorescence intensity was determined using FacsDiva software and converted to amount of antigen bound per cell.

Internalization assay

HT-29 human colon adenocarcinoma cells (ATCC) were seeded onto sterilized microscopy coverslips and grown in 24-well plates for 48 hours at 37°C in growth media. When approximately 50% confluent, the plates were placed on ice and the coverslips were washed twice with IF buffer (DPBS + 2% FBS). The primary antibody, MEN1309/OBT076 or human IgG H+L isotype control (R & D Systems) was diluted to 50 nmol/L in IF buffer and 200 μL were applied to the appropriate wells for 60 minutes on ice. Following primary antibody incubation, cells were washed twice with IF buffer. Secondary antibody (goat anti-human IgG, FITC, Southern Biotech) was diluted to a concentration of 50 nmol/L in IF buffer and 200 μL added to each well for 60 minutes on ice. The cells were washed, growth media was added to the wells, and the plate was returned to 37°C for the indicated amounts of time. For processing, the cells were washed twice with IF buffer and fixed in 2% paraformaldehyde (Affymetrix) on ice for 30 minutes. The coverslips were then air dried and mounted onto glass microscopy slides with a drop of Prolong Gold Anti-Fade Reagent plus DAPI (Invitrogen) as a nuclear counter stain. The cells were imaged and analyzed by fluorescent microscopy.

Cytotoxicity assay

Tumor cells were incubated with MEN1309/OBT076 for 72 hours at 37°C. Cell viability was measured by alamarBlue Cell Viability Reagent (Thermo Fisher Scientific) according to the manufacturer's instructions. Cells were incubated for 4 hours at 37°C with alamarBlue, and fluorescence was measured with an

Published OnlineFirst June 21, 2019; DOI: 10.1158/1535-7163.MCT-18-0624

Infinity 200 Plate Reader (Tecan). Percent viability was calculated using wells incubated in the absence of ADC as the control and was plotted versus antibody concentration. Nonlinear regression, sigmoidal dose-response analysis using GraphPad Prism Software (GraphPad) was used to calculate EC_{50} for each assay.

In vivo studies

The *in vivo* human tumor cell line xenograft studies were performed at Menarini Ricerche facilities, Charles River Discovery Research, or Washington Biotechnology. The athymic female nude mice (outbred, CD-1/nude) or female FOX Chase SCID (CB17/Icr-*Prkdcscid*/IcrIcoCrl) 5–8 weeks old, was purchased from Charles River and maintained in microisolator cages under continuously monitored environmental conditions. Drinking water and specific sterilized diet (VRF1, Charles River) were supplied *ad libitum*. Environmental conditions, as well as the procedures for housing and handling the animals, were in compliance with the United Kingdom Coordinating committee on Cancer Research guidelines (20) and the European Convention for the protection of vertebrate animals used for experimental and other scientific purposes (21) or the Association for Assessment and Accreditation of Laboratory Animal Care International.

A total of 5×10^6–2×10^7 cells with or without Matrigel, were injected subcutaneously into the flanks of mice. Tumor growth was followed by caliper measurement of length and width several times weekly. Tumor volume (expressed as mm^3) was calculated using the following formula: length (mm) $\times$ width^2 (mm)/2.

The body weight of mice was also monitored. The treatments were started when average tumor volume reached 88–300 mm^3. Animals were randomly assigned into groups (6 mice/group), and treated with MEN1309/OBT076 intravenously either with a single dose, once weekly for 2 consecutive weeks, or every 3 weeks for 3 consecutive weeks (q21dx3). The dose of MEN1309/OBT076 administered to mice ranged from 1.25 to 10 mg/kg. Tumor volume inhibition % in treated versus control mice was determined after the last drug treatment and at the nadir of tumor volume. Mice were euthanized when tumors reached 2,000 mm^3 or when the study endpoint was reached.

The antitumor activity of MEN1309 on patient-derived xenograft (PDX) models was carried out at the Lab Animal Service at Campus Vall d'Hebron Animal Facility by the Growth Factors laboratory of Vall D'Hebron Institute of Oncology (Barcelona, Spain) and at Champions Oncology, Inc. (see details in Supplementary Materials and Methods). The murine response criteria (mRECIST) used, follows the modified RECIST (22). The mRECIST criteria were applied only to mice that completed the efficacy study, while mice sacrificed earlier (for either ethical or pharmacodynamic reasons) were not included.

Mouse pharmacokinetics design

The tumor bearing and nontumor bearing mice were treated with a single intravenous administration of MEN1309/OBT076 at 5 mg/kg and sacrificed after 5 minutes, 30 minutes, 1 hour, 3 hours, 24 hours, 48 hours, 72 hours, 96 hours, 144 hours, 192 hours, 240 hours, 288 hours, 384 hours, 504 hours, 672 hours, and 816 hours, at which times samples (whole blood, tumor mass, and liver) were harvested. Three mice were used for each timepoint. To obtain the serum sample from the whole blood, the samples were left on the bench for 30 minutes at room temperature, to complete the coagulation process and then they were centrifuged at 3,000 rpm for 10 minutes at room temperature. We collected 250 μL of serum from each blood sample and stored it at −80°C.

MEN1309/OBT076 serum determination in mice

An indirect ELISA system was used. The plate coating was performed using 100 μL/well of 2 μg/mL of CD205 antigen (OBT076ECD) solution. The plate was covered and stored at +4°C for at least 12 hours and at the most for 3 days. After coating, the plate was washed for three times with 300 μL/well of PBS 1X 0.05% Tween-20, then each well was blocked with 200 μL of PBS 1X, 0.05% Tween-20–2% BSA. The plate was covered and incubated under stirring (350 rpm) for 2 hours at room temperature. After blocking, the plate was washed for three times with 300 μL/well of PBS 1X 0.05% Tween-20, then 100 μL of each sample were plated in duplicate, following the daily scheme. The plate was covered and incubated under stirring (350 rpm) for one hour at 37°C. Then, the plate was washed for three times with 300 μL/well of PBS 1X, 0.05% Tween-20 and incubated with 50 μL of Biotin Anti maytansine antibody 50 ng/mL under stirring (350 rpm) for one hour at 37°C. Following the Biotin anti maytansinoid antibody linkage, the plate was washed for three times with 300 μl/well of PBS 1X, 0.05% Tween-20, then each well was filled with 100 μL of Strepatvidin poly-HRP40 conjugated diluted 1:10000. The plate was covered and incubated under stirring (350 rpm) for one hour at 37°C. Then, the plate was washed for three times with 300 μL/well of PBS 1X, 0.05% Tween-20 and 100 μL of the TMB was added. The plate was covered and incubated without stirring at 37°C for 10 minutes. The enzymatic reaction was stopped by adding 100 μL/well of 1 N HCl, and then the plate was immediately read.

Phospho-histone H3 immunofluorescence

Tumor mass sections were incubated in permeabilization buffer (PBS + 1% BSA + 0.3% Triton × −100) for 30 minutes at room temperature, then blocked in PBS (5% normal goat serum + 1% BSA) for 1 hour at room temperature. Tumor mass sections were then incubated with rabbit polyclonal (Abcam ab47297) anti-phospho (phospho S10) histone H3 diluted 1:1,000 in blocking buffer (5% normal goat serum + 1% BSA in PBS) overnight at 4°C. After 3 × 5 minutes washes with PBS, the slides were incubated with goat anti-rabbit secondary antibody, Alexa 594 (R37117) for 1 hour at room temperature. After 3 × 5 minutes washes with PBS, the slides were mounted in Vectashield (H-1200, Vector Laboratories) with DAPI (4′, 6-diamidin-2-fenilindolo). The stained sections were visualized with a Leitz Diaplan fluorescent microscope and the images were captured with a Leica DFC450 C camera at 25×. The images were exported from the Leica software and analyzed using ImageJ software. Each image was converted to "binary" color. Nonspecific signals and background were removed using the program function "Despeckly". The "Withwater" function was used to divide the adjacent nuclei. The "analyze particles" function was used to count the total nuclei in the image and "250-infinity" was used to limit the size. The positive cells were counted manually with the function "cell counter".

Statistical analyses

GraphPad Prism Software (GraphPad Software Inc.) was used for statistical analysis. Statistical differences were considered to be significant at $P < 0.05$ using the two-tailed Mann–Whitney rank test. *In vivo* data are presented as mean, with the value for each

Published OnlineFirst June 21, 2019; DOI: 10.1158/1535-7163.MCT-18-0624

group represented as a symbol of different shape and line of different color.

Results

CD205 expression in human solid tumors of different histotypes

Using the OGAP target discovery system and proteomic analysis, we identified CD205 antigen as highly expressed in a range of solid tumors (gastric, pancreatic, bladder, breast, and colon) and hematologic lymphomas [multiple myeloma and diffuse large B-cell lymphoma (DLBCL)]. Pancreatic cancer, triple-negative breast cancer (TNBC), and DLBCL displayed particularly high levels of CD205 (Fig. 1A). In fact, mass spectrometry of tumor cell membranes demonstrated that CD205 expression was elevated in pancreatic cancer compared with normal pancreas, and in TNBC compared with other breast cancer types (Fig. 1B). We confirmed and extended these initial proteomic observations by using a specific antibody against CD205 for IHC evaluation of the protein expression in many different solid tumor types. We found CD205 expression to vary in abundance frequency, depending on the specific cancer type examined (Supplementary Table S1). Consistent with the proteomics data, strong and specific CD205 staining was detected in TNBC (75% prevalence), bladder cancer (70% prevalence), and pancreatic tumors (68% prevalence), whereas it was much reduced in the corresponding normal tissues using a commercial CD205 antibody (Fig. 1C; Supplementary Table S2). Because target expression on normal tissues should be little to limit the on-target off-tumor toxicity events, we

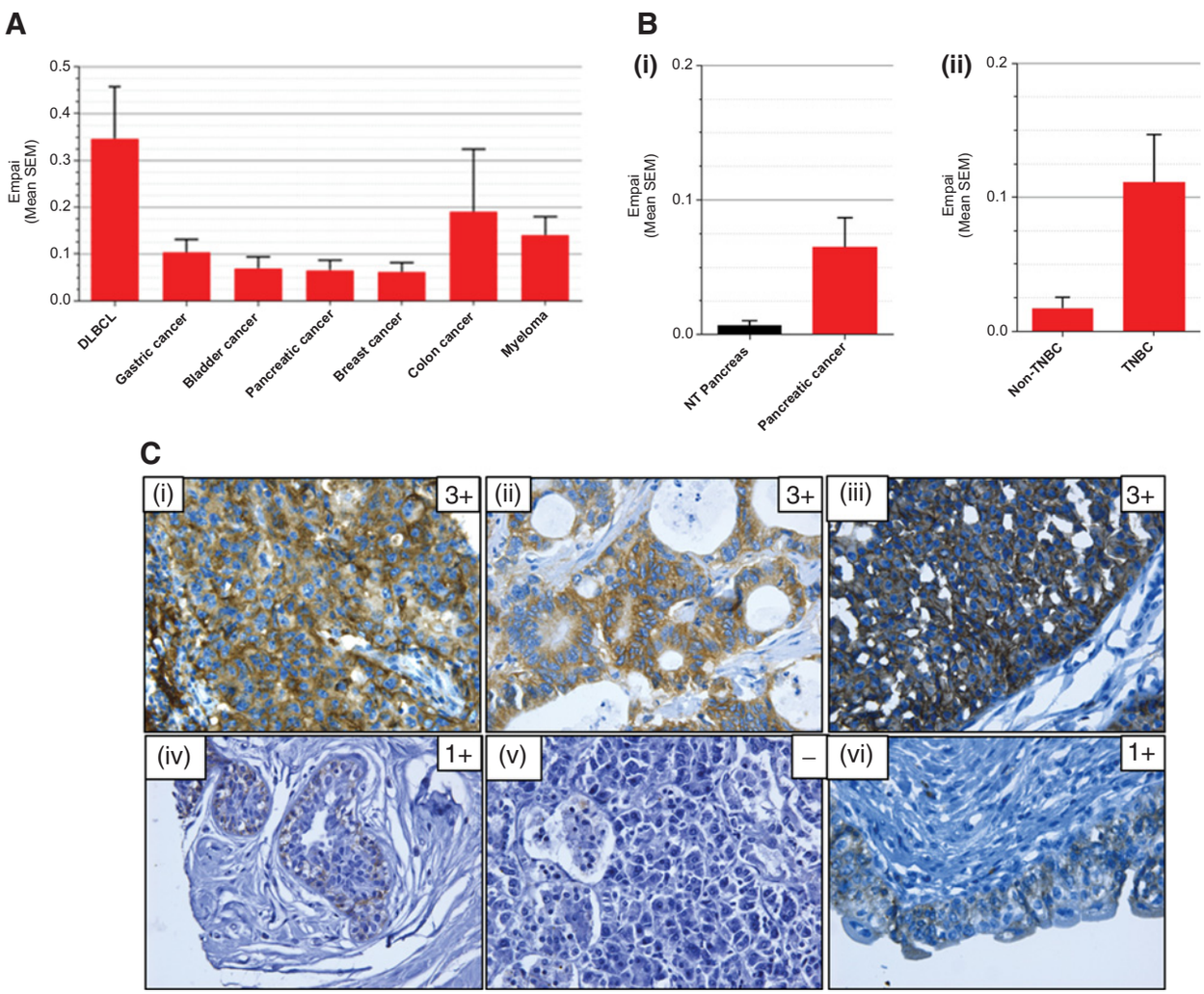

Figure 1.

A, The mean proteomic expression of CD205 in multiple solid tumors and hematologic malignancies is shown. **B,** The differential expression of CD205 in different tumor types compared with their normal tissue counterpart or other tumor subtypes as assessed by proteomics analysis is shown in pancreatic tumors ($n = 10$) compared with normal pancreas ($n = 3$; i) and in TNBC ($n = 3$) compared with non-TNBC ($n = 4$; ii). **C,** Representative photomicrograph images depict the differential expression of CD205 in breast cancer (i), pancreatic cancer (ii), and bladder cancer (iii) compared with the corresponding normal tissues of breast (iv), pancreas (v), and bladder (vi) as assessed by IHC. Staining intensity (scored on a 0–3+ scale) is indicated in the top right of each panel. All images are shown in 40× magnification.

Published OnlineFirst June 21, 2019; DOI: 10.1158/1535-7163.MCT-18-0624

performed a GLP tissue cross reactivity study, based on IHC staining, with a panel of 33 different frozen human and cynomolgus monkey tissues and blood smears. Tissue sections incubated with MEN1309/OBT076, showed a specific membranous/cytoplasmic staining of mononuclear cells (like an admixture of dendritic/B-like and lymphocytes), in several tissues, including thymus, lymph node, and spleen. No differences between human and cynomolgus samples were observed (Supplementary Fig. S1). The lack of significant cross-reactivity of MBH1309/OBT076 to the rat and mouse antigen coupled to the comparable human and cynomolgus binding activity (Supplementary Table S3), support the latter as relevant animal species for predictive clinical toxicity. We developed a fully human IgG1 mAb (MBH1309/OBT076), which specifically binds to CD205. Using immunofluorescence microscopy, we assessed the localization of CD205 expression in tumor cells over time. Intact, live CD205-positive HT-29 colon cancer cells were labeled with MBH1309/OBT076 under low temperature conditions that restrict internalization. Accordingly, a positive signal for the CD205–MBH1309/OBT076 complex was concentrated at the plasma membrane of the cells (Fig. 2). In contrast, under high temperature conditions that permit internalization, cytoplasmic puncta were observed after 5–15 minutes and a complete relocalization of the signal from the cell periphery to the cell interior was apparent after 60 minutes. These data indicate that CD205 undergoes efficient internalization following engagement by the MBH1309/OBT076 antibody, consistent with the reported kinetics of other antigen/antibody complexes (23–25).

The high medical need reported in those cancers showing a substantial prevalence of CD205 expression together with the ability of the antigen to efficiently internalize from the surface of cancer cells, suggested that an ADC directed toward CD205 might be an effective anticancer therapeutic strategy. On the basis of these considerations an ADC therapeutic development approach was initiated and two ADC formats were evaluated.

Development of the MEN1309/OBT076 ADC

The MBH1309/OBT076 human anti-CD205 antibody was initially conjugated to two different antibiotic agents, the maytansinoid DM1 and DM4 toxins, through a noncleavable MMC

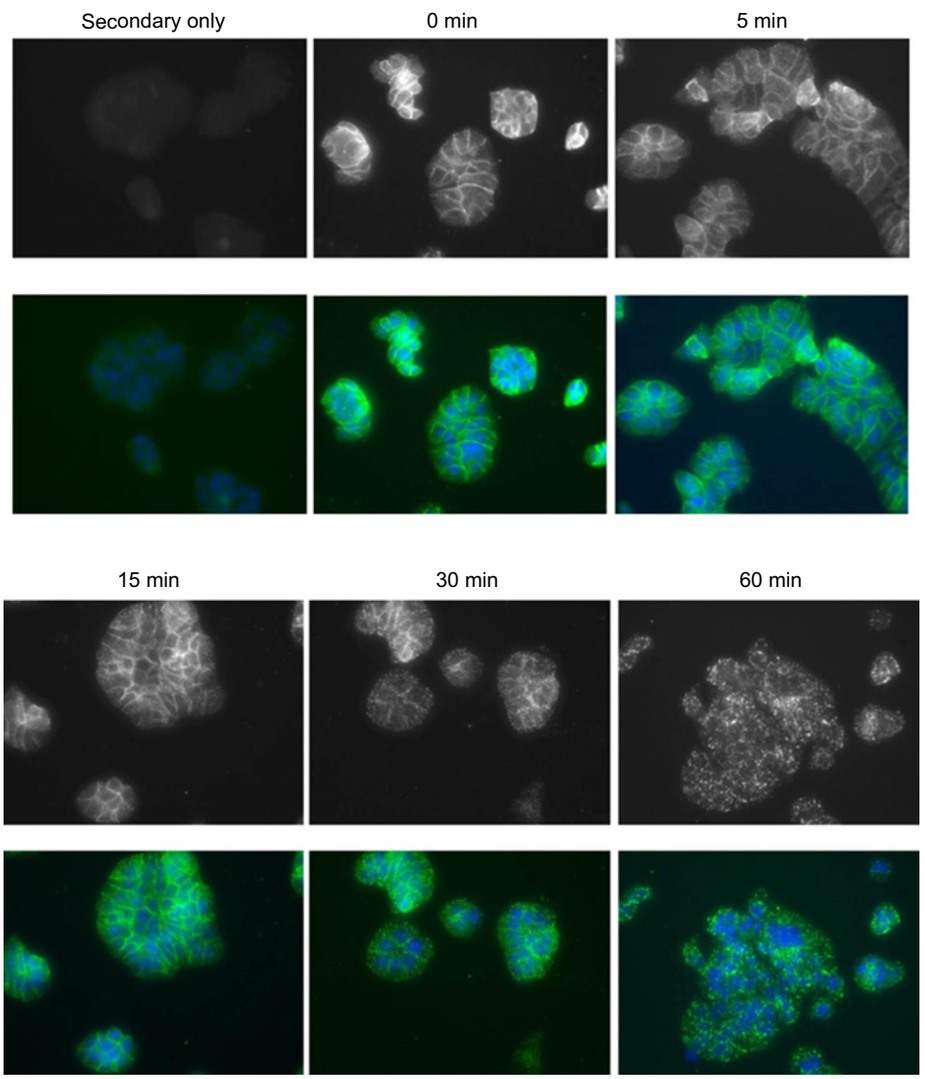

Figure 2.
Immunofluorescence analysis of MBH1309/OBT076 internalization from the surface of HT-29 cells. Representative images of HT-29 cells, labeled with secondary antibody only (control) or MBH1309/OBT076 antibody at 0, 5, 15, 30, and 60 minute timepoints after incubation at 37°C to allow internalization. Top row shows MBH1309/OBT076 fluorescence; bottom row shows merged images of MBH1309/OBT076 fluorescence (green) and DAPI (blue).

Published OnlineFirst June 21, 2019; DOI: 10.1158/1535-7163.MCT-18-0624

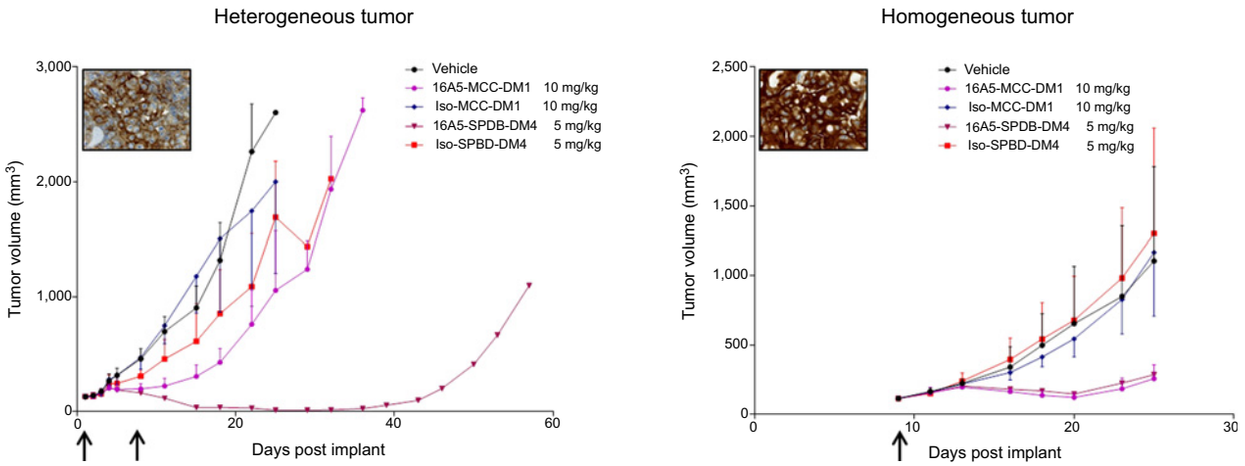

Figure 3.

MBH1309/OBT076-SPDB-DM4 and MBH1309/OBT076-MMC-DM1 antitumor activity on HPAFII xenograft tumors (showing homogenous staining for CD205; right) and Raji xenograft tumors (showing heterogeneous staining for CD205; left). Tumor volume versus time graphs is shown. Arrows indicate treatment administration. Insets are representative images of the CD205 staining in the vehicle-treated group of animals.

(4-[N-maleimidomethyl] cyclohexane-1-carboxylate) linker and a cleavable SPDB linker, respectively. The antitumor activity of the ADCs was then evaluated in solid and hematologic mouse xenograft models. The ADCs showed comparable *in vivo* antitumor activity against the HPAFII pancreatic cancer xenograft tumor model (Fig. 3B) exhibiting homogeneous expression of the target antigen as shown by IHC, whereas, in the Raji DLBCL xenograft tumor model (Fig. 3A) with heterogeneous expression of the CD205 antigen, the *in vivo* efficacy of MBH1309/OBT076-SPDB-DM4 (reported as 16A5-SPDB-DM4 in Fig. 3) administrated at 5 mg/Kg was much more potent than that of MBH1309/OBT076-MMC-DM1 (reported as 16A5-MMC-DM1 in Fig. 3) administrated at 10 mg/Kg (Fig. 3A and B).

On the basis of these data, MBH1309/OBT076-SPDB-DM4 (designated MEN1309/OBT076 from here on) was selected as a lead candidate ADC to target CD205-positive cancers.

In vitro characterization

The expression of the CD205 antigen was evaluated in a panel of human pancreas, bladder, colon cancer, and TNBC cell lines. The expression level of CD205 mRNA was evaluated by real-time quantitative PCR (qRT-PCR), whereas the expression of the protein was characterized by IHC staining and the surface localization of the protein was determined by FACS.

The expression of the CD205 antigen in the analyzed cancer cell lines was quite heterogeneous; within each histotype the antigen expression ranged from strongly positive to completely negative. The expression data results were very consistent among the three different techniques and in all cases the highest expression level of the CD205 antigen was observed in several pancreatic and TNBC cell lines. The pancreas, bladder, colon cancer, and TNBC cell lines were used as *in vitro* models to assess the cytotoxic activity of MEN1309/OBT076. The ADC showed a potent cytotoxic effect on antigen-positive cells, with EC_{50} values between 0.1 and 1.32 nmol/L. Moreover, the antiproliferative impact of the ADC was demonstrated against cell lines expressing the antigen at high as well as at low to moderate levels. On the contrary, MEN1309/OBT076 showed a negligible effect on CD205-negative cells (Table 1).

We also assessed MEN1309/OBT076 for its binding affinity to the CD205 antigen on the THP1 cell line (Supplementary Fig. S2B), as well as its affinity to the FcγRIIIA receptor (Supplementary Fig. S2A) and propensity for participation in putative alternative mechanisms of action such as antibody-dependent cellular cytotoxicity (ADCC). Indeed, MEN1309/OBT076 showed the ability to bind to FcγRIIIA, but no ADCC response was reported as consequence nevertheless the data might not support ADCC activity of MEN1309/OBT076 at least *in vitro* (Supplementary Fig. S2C). The ability of the antibody to mediate a CDC response was also investigated and no evidence of such activity was observed (Supplementary Fig. S2D). These data suggest that the therapeutic efficacy of MEN1309/OBT076 may rely primarily on an ADC-based mechanism of action (Supplementary Fig. S2).

MEN1309/OBT076 *in vivo* efficacy in CD205-expressing xenografts and PDX models

To test the *in vivo* efficacy of MEN1309/OBT076, different xenograft and PDX models were selected on the basis of the IHC analysis for CD205 staining in various tumor types (Supplementary Table S4). Efficacy of MEN1309/OBT076, administered with a q21dx3 schedule, was determined by assessing the inhibition of tumor growth at the nadir of tumor volume in treated versus control mice and assessing mRECIST criteria adapted to the mouse from human RECIST (26). No toxic effects of MEN1309/OBT076 were observed in any of the studies.

TNBC. In two xenograft models of TNBC, HCC-1806 and HCC-70, classified as low antigen–expressing cell lines by IHC (score of 1+), MEN1309/OBT076 showed an impressive antitumor activity (Fig. 4A and B). In both models, 5 mg/kg MEN1309 resulted in complete tumor regression in all the treated animals (5/5). The MEN1309/OBT076-mediated reduction in tumor growth was dose dependent. Antitumor activity was also observed at

Published OnlineFirst June 21, 2019; DOI: 10.1158/1535-7163.MCT-18-0624

Table 1. MEN1309/OBT076 cytotoxicity and CD205 expression in human cancer cell lines

Cell line	Tissue	EC_{50} (nmol/L)	qRT-PCR (RCN)	FACS (No. antigen per cell)	IHC Score (Cell block)
HPAFII	Pancreas	0.10	0.95	44,576	+++
THP-1	Peripheral blood	–	0.66	17,205	++
HT29	Colon	0.40	0.53	49,765	+++
HCC-1806	Breast (TNBC)	0.81	0.38	7,337	+
BxPC3	Pancreas	0.43	0.35	–	+++/++
HCC-70	Breast (TNBC)	0.71	0.26	–	++/+
SW780	Urinary bladder	0.26	0.23	8,000	++
SU.86.86	Pancreas	1.32	0.22	26,781	++/+
5637	Urinary bladder	–	0.17	–	–
HCC-1143	Breast (TNBC)	0.82	0.12	–	++/+
MDA-MB-468	Breast (TNBC)	0.37	0.12	–	+++
MDA-MB-231	Breast (TNBC)	–	0.057	–	–
TOLEDO	Peripheral blood	–	0.05	798	–
HT1376	Urinary bladder	–	0.05	–	0
ScaBER	Urinary bladder	–	0.04	–	0
AspC1	Pancreas	22.66	<0.01	1,305	0
BT-20	Breast (TNBC)	–	<0.01	–	–
TCC-SUP	Urinary bladder	–	<0.01	–	–
HT1197	Urinary bladder	36.23	<0.01	–	0
MCF-7	Breast	14.20	<0.01	–	0
UMUC3	Urinary bladder	–	<0.01	–	0

NOTE: The expression of CD205 was characterized in a panel of human cancer cell lines of different histotypes. qRT-PCR was used to evaluate the expression level of CD205 mRNA, and the results were expressed as RCN. The expression level of CD205 protein was determined by measuring the number of surface antigen per cells using quantitative FACS and assessing the antigen expression in tissue sections by IHC staining. –, not tested; 0, no staining; +, weak staining; ++, moderate staining; +++, strong staining.
Abbreviation: RCN, relative copy number.

2.5 mg/kg, with a complete response in 60% of the mice carrying HCC-1806 tumors (3/5), and in 80% of treated mice carrying HCC-70 tumors (4/5), according to mRECIST criteria (Fig. 4A and B). Unexpectedly, the administration of IgG1-DM4 control ADC showed a very slight effect on tumor growth.

IHC for CD205 expression evaluated on the residual tumor masses 16 days after the first treatment showed that, in the HCC-1806 xenograft model, all doses of MEN1309/OBT076 eliminated antigen-positive tumor cells, whereas in the HCC-70 xenograft model, low antigen expression persisted in the tumor cells from all treated groups (Supplementary Fig. S3A).

Furthermore, the antitumor activity of MEN1309/OBT076 was also evaluated in PDX models of TNBC. As shown in Fig. 5A, MEN1309/OBT076 demonstrated significant antitumor activity against the PDX-347 model, characterized by strong (score of 3+) and homogenous CD205 tumor staining. Importantly, at study endpoint, 4 of 6 mice (66%) treated with 5 mg/kg MEN1309/OBT076 had a long lasting complete response (mCR) according to mRECIST criteria. IHC on tumor tissue samples after two treatments revealed that the tumors were composed of fibrotic tissue and few cells with a moderate expression of target antigen (Supplementary Fig. S3B). Positive, although less robust results were also observed on the PDX-22 model scoring 1+ level of the CD205 antigen (Fig. 5B).

Pancreatic cancer. In HPAFII, a xenograft model of pancreatic adenocarcinoma, in which tumors exhibited strong CD205 expression (scored as 3+ by IHC), potent MEN1309/OBT076-mediated antitumor activity was observed in mice treated with at least 5 mg/kg of the ADC (Fig. 4C). Complete regressions were observed in 50% of the treated mice. On the contrary, no activity was observed in the AsPC-1 pancreatic adenocarcinoma xenograft model, characterized by lack of CD205 antigen expression (Fig. 4D).

In PDX-21, a PDX pancreatic cancer model with weak and heterogeneous CD205 expression, treatment with 5 mg/kg MEN1309/OBT076 resulted in a complete response in 1 of 6 mice and a partial response in 1 of 6 mice according to mRECIST criteria (Fig. 5C). This efficacy is encouraging, although more modest as compared with that seen in PDX models with high expression of the CD205 antigen (Fig. 5D).

Bladder cancer. In the human bladder carcinoma SW780 xenograft model (scored as 2+ for CD205 by IHC), MEN1309/OBT076 was able to induce a complete response in all mice treated at 10 and 5 mg/kg and in half (2/4) of the mice treated with 2.5 mg/kg. The mRECIST evaluation indicated a complete response score from 5 mg/Kg (Fig. 4E). More modest findings with similar trends were observed in PDX models (Fig. 5E and F). In contrast, free DM4 toxin administered at an equimolar concentration (200 μg/kg) of MEN1309/OBT076 showed no activity (Fig. 4E).

Pharmacokinetics, pharmacodynamics, and toxicity profiling of MEN1309/OBT076

The pharmacokinetics profile of MEN1309/OBT076 was analyzed after single intravenous administration at 5 mg/Kg in HPAFII pancreatic xenograft–bearing mice (characterized by a strong CD205 expression and 3+ IHC score), when average tumor volume reached 200 mm^3, and in nontumor-bearing mice. The associated pharmacodynamics of the ADC was also analyzed. Because of the molecular mechanism of DM4, the phosphorylation of histone H3 on Serine10, was used as a biomarker of mitotic arrest in the tumor mass (27). The pharmacokinetic profile of MEN1309/OBT076 was comparable in tumor-bearing and in tumor-free mice (Fig. 6A) and the serum concentration of the ADC over time was as expected and similar to that seen for other ADCs (28). Importantly, the pharmacokinetics of

Published OnlineFirst June 21, 2019; DOI: 10.1158/1535-7163.MCT-18-0624

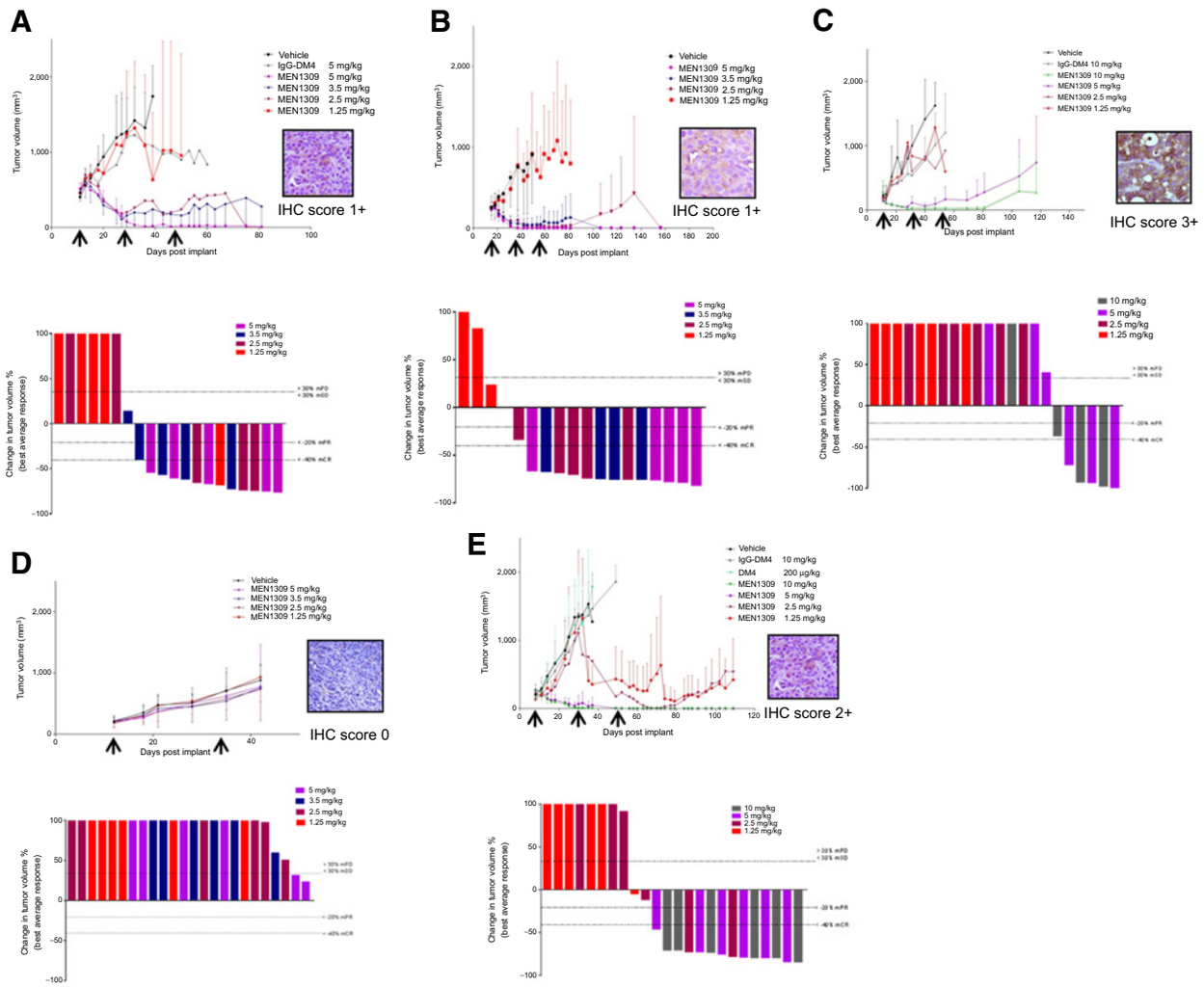

Figure 4.

MEN1309/OBT076 antitumor efficacy against human TNBC (**A** and **B**), pancreatic (**C** and **D**), and bladder (**E**) cancer xenograft models. HCC-1806 (**A**); HCC-70 (**B**); HPAFII (**C**); AsPC-1 (**D**); and SW780 (**E**) tumor cell lines. For each tumor model, the IHC staining and scoring, tumor growth curves in response to the treatments, and waterfall plot response to the MEN1309/OBT076 according to mRECIST criteria at 1 week after the last treatment are shown. Each bar represents a single mouse. mCR, complete response; mPD, progressive disease; mPR, partial response; mSD, stable disease.

the ADC concentration in the serum correlated with the kinetics of antitumor efficacy observed in this xenograft model. By immunofluorescence labeling of phospho-histone H3, a significant antimitotic effect of the ADC was observed (Fig. 6A and B). The fluorescent-positive cells (indicative of mitotic arrest) increased in the tumor mass in parallel with the reduction of tumor growth and correlated with the serum concentration of MEN1309/OBT076. A maximum level of phosphorylated H3 in tumor cells mass was obtained 96 hours after MEN1309/OBT076 administration. MEN1309/OBT076 GLP toxicity studies (Supplementary Table S5) performed on cynomolgus monkeys showed minimal antigen staining in the bone marrow, blood samples, and respiratory system and lack of CD205 positivity in the skin. The main finding observed following either single or repeated MEN1309/OBT076 administration was a slight nongender-related neutropenia, a quite common adverse event for ADCs.

Discussion

An increasing number of ADCs in clinical development highlight the continued interest in this type of targeted therapy, which exploits the specificity of tumor-associated antigens to distribute potent cytotoxic agents to solid and hematologic tumors. In this work, we present the preclinical antitumor profile of the first-in-class ADC, MEN1309/OBT076, targeting tumors expressing the CD205 antigen. The payload DM4 is a maytansine derivative endowed with potent antimitotic effects due to its ability to inhibit microtubule assembly at nanomolar concentrations (17, 18).

The CD205 antigen, a transmembrane protein member of the macrophage mannose receptor family of C-type lectins, is an ideal target for an ADC-based therapy because it is highly overexpressed in different solid tumors compared with healthy tissues. Antigen positivity observed in dendritic cells is not

Published OnlineFirst June 21, 2019; DOI: 10.1158/1535-7163.MCT-18-0624

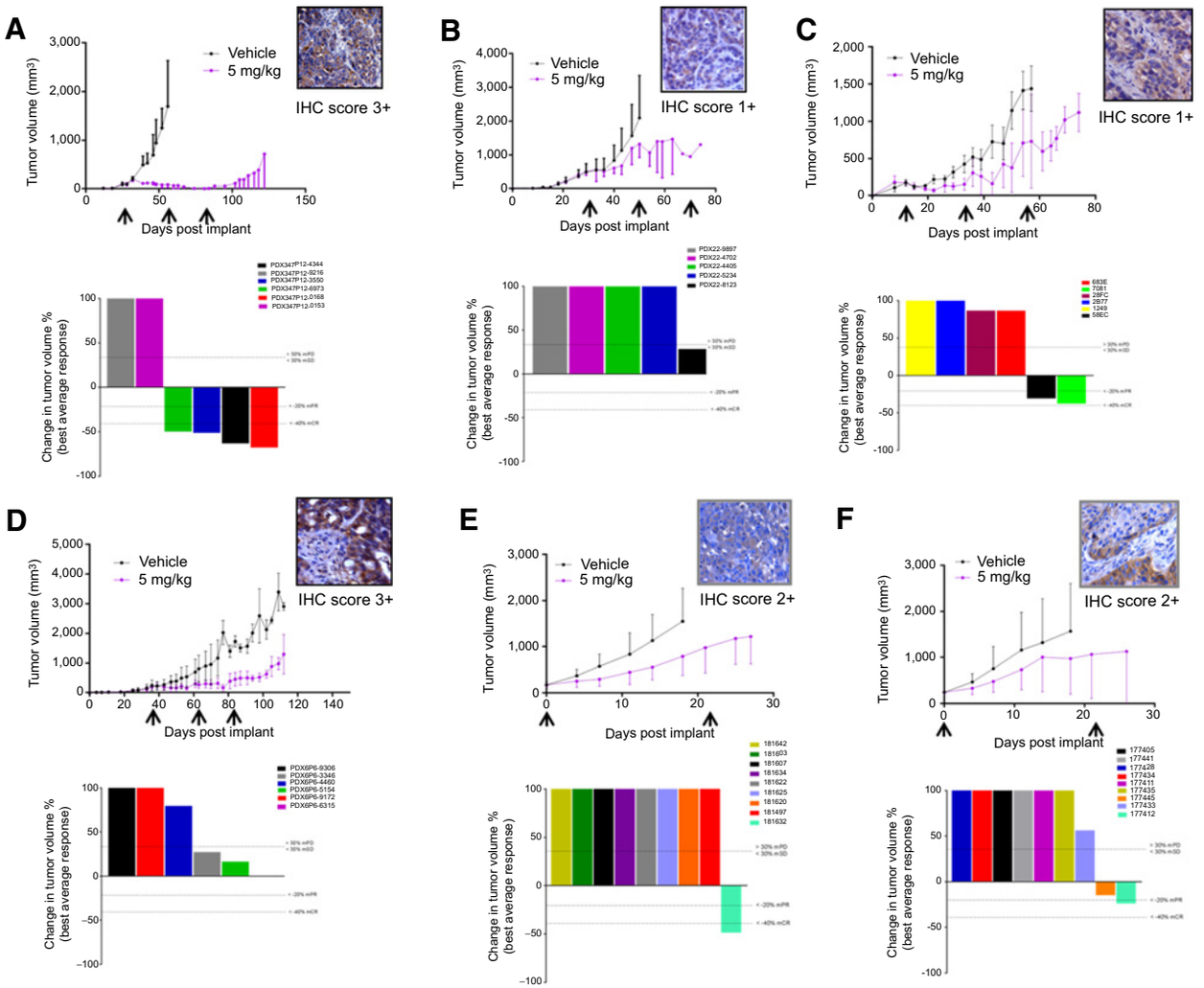

Figure 5.

MEN1309/OBT076 antitumor efficacy against human TNBC (**A** and **B**), pancreatic (**C** and **D**), and bladder (**E** and **F**) cancer PDX models. PDX-347 (**A**); PDX-22 (**B**); PDX-21 (**C**); PDX-P6P (**D**); PDX-CTG-1388 (**E**); and PDX-CTG-1652 (**F**) PDX models. For each PDX model, the IHC staining and scoring, tumor growth curves in response to the treatments, and waterfall plot response to the MEN1309/OBT076 according to mRECIST criteria at 1 week after the last treatment are shown. Each bar represents a single mouse. mCR, complete response; mPD, progressive disease; mPR, partial response; mSD, stable disease.

hypothesized to have a major impact on their potential antitumor immunity activity, due to the suggested nonendocytic function of CD205 expressed on mature dendritic cells (29). Moreover based on their low proliferation index, they should be spared by the cell killing activity exerted by the maytansinoid derivate payload. In addition, CD205 exhibits a rapid internalization rate, which allows the efficient delivery of the cytotoxic payload into the target cells. The fast antigen/antibody complex internalization rate observed (a remarkable amount of relocalized antibody was already apparent after 30 minutes of cells labeling), might suggest that the antibody is not bound to the membrane long enough to mount a detectable ADCC or CDC activity in a cell-based assay which lasts for hours. However, the contribution of the immune activation functions, in terms of cell killing, would be quite limited compared with the cytotoxic potential mediated by the ADC payload.

Here, we demonstrated that the conjugation of MBH1309/OBT076 with the DM4 toxin through a cleavable SPDB linker was the most effective construct in terms of antitumor activity. In fact, the conjugation of DM4 through a noncleavable linker was less active in tumors with a heterogeneous expression of the antigen. The cleavable linker allows the bystander killing effect to eliminate antigen-negative tumor cells (30). Indeed, MEN1309/OBT076 demonstrated a cytotoxic activity in the picomolar range against cells having strong (IHC score of 3+) to weak (IHC score of 1+) antigen expression. A negligible effect was observed on CD205 antigen–negative cells, thus highlighting the specificity of this ADC.

On the basis of these data, we developed MEN1309/OBT076 for clinical use. MEN1309/OBT076 showed a remarkable antitumor activity in a panel of xenograft and PDX tumor models of TNBC (Figs. 4 and 5; Supplementary Table S3).

Published OnlineFirst June 21, 2019; DOI: 10.1158/1535-7163.MCT-18-0624

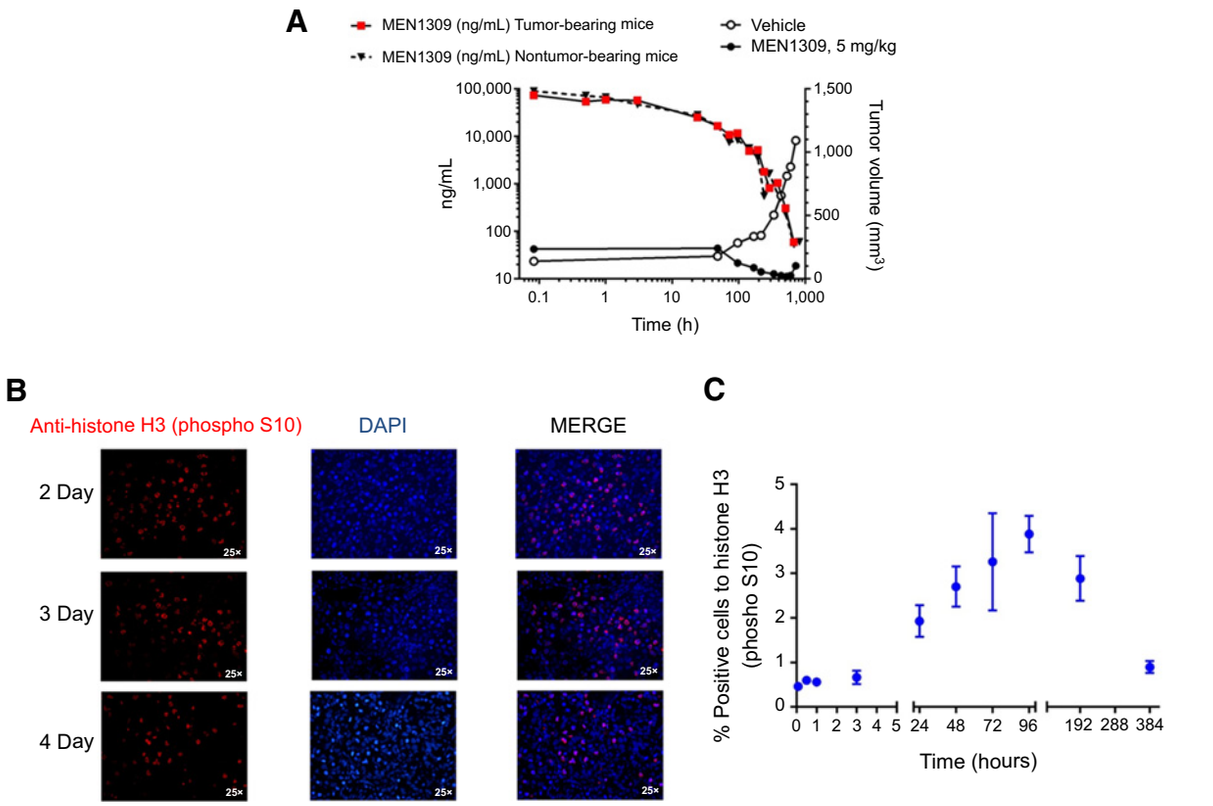

Figure 6.

A, Serum concentration versus time profile of MEN1309/OBT076 in tumor-bearing (red square) and nontumor-bearing (black triangle) mice associated with the antitumor activity of MEN1309/OBT076 on HPAFII human pancreatic carcinoma xenograft model: open circle, tumor growth in the vehicle, and black circle, in MEN1309/OBT076-treated mice. **B,** IF labeling of HPAFII human pancreatic tumor sections at different timepoints after MEN1309/OBT076 treatment. Alexa 594 (red) nuclear histone H3 phosphorylated on serine10 (H3pS10); DAPI nuclear labeling (blue); and MERGE. **C,** Percentage of histone H3pS10–positive cells in HPAFII tumor sections versus time posttreatment with MEN1309/OBT076.

Interestingly, in two xenograft models of TNBC expressing low CD205 antigen (weak staining with 1+ IHC score), 2.5 mg/Kg of MEN1309/OBT076 was able to completely inhibit the tumor growth. A compelling *in vivo* efficacy was observed also on TNBC PDX models expressing the antigen at high levels. Furthermore, 5 mg/kg of MEN1309/OBT076 also induced complete responses in the HPAFII pancreatic cancer xenograft model.

Treatment of the low antigen–expressing SW780 bladder cancer xenograft model with MEN1309/OBT076 produced a good response, whereas the efficacy was reduced when we treated the bladder PDX models expressing intermediate antigen levels.

Overall, comparing the activity of MEN1309/OBT076 in TNBC to that in pancreatic cancer, it is clear that the antigen expression level is not the sole factor contributing to the ADC-mediated tumor cell cytotoxicity; the sensitivity of the tumor histotype to the toxin, the internalization rate, and the cellular metabolism, appear to play important roles in the antitumor efficacy of the compound. As a whole, these data suggest that the antigen expression is necessary but not sufficient for significant antitumor activity of MEN1309/OBT076.

The pharmacokinetic/pharmacodynamic experiment conducted on the HPAFII pancreatic xenograft model indicates that the serum concentration of MEN1309/OBT076 positively correlates with the tumor growth inhibition observed. Interestingly, no difference was found between the MEN1309/OBT076 serum pharmacokinetic profile in tumor-bearing and nontumor-bearing mice, suggesting that tumor cells highly expressing CD205 do not act as a substantial sink for the ADC.

Moreover, the time course of histone H3 phosphorylation (a pharmacodynamic marker of DM4 activity) in the HPAFII tumor mass showed a significant gradual increase of mitotically arrested cells up to 96 hours after MEN1309/OBT076 administration. Importantly, the onset of the antitumor effect was concurrent with the peak of histone H3 phosphorylation.

Overall, the data presented here demonstrate that MEN1309/OBT076 is a selective and promising first-in-class antitumor ADC. Together with an acceptable toxicity profile in relevant preclinical species, these data supported the start of the first-in-human SHUTTLE study (NCT03403725) in patients with CD205-positive metastatic solid tumors and relapsed or refractory non-Hodgkin lymphoma.

Disclosure of Potential Conflicts of Interest

J. Arribas is a consultant/advisory board member for Menarini Biotech. C.M. Lynch is senior vice president, nonclinical development, at and is a consultant/advisory board member for Oxford Biotherapeutics. C. Rohlff has ownership interest (including stock, patents, etc.) in Oxford Biotherapeutics. A. Pellacani is head of research and development at Menarini Ricerche and has ownership

interest (including stock, patents, etc.) in Amgen. No potential conflicts of interest were disclosed by the other authors.

Authors' Contributions

Conception and design: A. Fiascarelli, M. Bigioni, R.L. Dusek, D. Aud, C.M. Lynch, J. Terrett, K.E. Wilson, C. Rohlff, A. Pellacani, M. Binaschi
Development of methodology: G. Merlino, A. Fiascarelli, M. Bigioni, C. Carrisi, R. Bugianesi, R. Manno, R. Awdew, D. Aud, C.M. Lynch
Acquisition of data (provided animals, acquired and managed patients, provided facilities, etc.): G. Merlino, M. Bigioni, C. Carrisi, C. Bernadó Morales, J. Arribas, R.L. Dusek, P.H. Pham, R. Awdew, D. Aud, M. Trang
Analysis and interpretation of data (e.g., statistical analysis, biostatistics, computational analysis): G. Merlino, A. Fiascarelli, M. Bigioni, A. Bressan, C. Carrisi, D. Bellarosa, R. Bugianesi, C. Bernadó Morales, J. Arribas, R.L. Dusek, J.E. Ackroyd, P.H. Pham, D. Aud, M. Trang, C.M. Lynch, A. Pellacani
Writing, review, and/or revision of the manuscript: G. Merlino, A. Fiascarelli, M. Bigioni, A. Bressan, M. Salerno, R. Bugianesi, J. Arribas, R.L. Dusek, C.M. Lynch, S. Manzini, A. Pellacani, M. Binaschi
Administrative, technical, or material support (i.e., reporting or organizing data, constructing databases): G. Merlino, M. Bigioni, R. Manno, P.H. Pham, S. Manzini
Study supervision: M. Bigioni, R.L. Dusek, K.E. Wilson, S. Manzini

The costs of publication of this article were defrayed in part by the payment of page charges. This article must therefore be hereby marked *advertisement* in accordance with 18 U.S.C. Section 1734 solely to indicate this fact.

Received July 10, 2018; revised January 16, 2019; accepted June 17, 2019; published first June 21, 2019.

References

1. Jerjian TV, Glode AE, Thompson LA, O'Bryant CL. Antibody-drug conjugates: a clinical pharmacy perspective on an emerging cancer therapy. Pharmacotherapy 2016;36:99–116.
2. Diamantis N, Banerji U. Antibody-drug conjugates: an emerging class of cancer. Br J Cancer 2016;114:362–7.
3. Perez HL, Cardarelli PM, Deshpande S, Gangwar S, Schroeder GM, Vite GD, et al. Antibody–drug conjugates: current status and future directions. Drug Discov Today 2014;19:869–81.
4. Lambert JM. Drug-conjugated antibodies for the treatment of cancer. Br J Clin Pharmacol 2013;76:248–62.
5. Hedrich WD, Fandy TE, Ashour HM, Wang H, Hassan HE. Antibody-drug conjugates: pharmacokinetic/pharmacodynamic modeling, preclinical characterization, clinical studies, and lessons learned. Clin Pharmacokinet 2018;57:687–703.
6. Kast J, Boyd R, Ackroyd J, Allen J, Anderson A, Barnes M, et al. Abstract 3869: Proteomics highlights which G-protein coupled receptors are candidates for ADC development. In: Proceedings of the 103rd Annual Meeting of the American Association for Cancer Research; 2012 Mar 31–Apr 4; Chicago, IL. Philadelphia (PA): AACR; Cancer Res 2012;72(8 Suppl): Abstract nr 3869.
7. Taylor ME, Conary JT, Lennartz MR, Sthal PD, Drickamer K. Primary structure of the mannose receptor contain multiple motifs resembling carbohydrate-recognition domains. J Biol Chem 1990;265:12156.
8. Ezekowitz RA, Sastry K, Bailly P, Werner A. Molecular characterization of the human macrophage mannose receptor: demonstration of multiple carbohydrate recognition-like domains and phagocytosis of yeast in Cos-1 cells. J Exp Med 1990;172:1785.
9. Zelensky AN, Gready JE. The C-type lectin-like domain superfamily. FEBS J 2005;272:6179–217.
10. Bonifaz L, Bonnyay D, Mahnke K, Rivera M, Nussenzweig MC, Steinman RM. Efficient targeting of protein antigen to the dendritic cell receptor DEC-205 in the steady state leads to antigen presentation on major histocompatibility complex class I products and peripheral CD8+ T cell tolerance. J Exp Med 2002;196:1627.
11. Jiang W, Swiggard WJ, Heufler C, Peng M, Mirza A, Steinman RM, et al. The receptor DEC-205 expressed by dendritic cells and thymic epithelial cells is involved in antigen processing. Nature 1995;375:151–5.
12. Cao L, Shi X, Chang H, Zhang Q, He Y. pH-dependent recognition of apoptotic and necrotic cells by the human dendritic cell receptor DEC205. Proc Natl Acad Sci U S A 2015;112:7237–42.
13. Shrimpton RE, Butler M, Morel AS, Eren E, Hue SS, Ritter MA. CD205 (DEC-205): a recognition receptor for apoptotic and necrotic self. Mol Immunol 2009;46:1229–39.
14. Cao L, Chang H, Shi X, Peng C, He Y. Keratin mediates the recognition of apoptotic and necrotic cells through dendritic cell receptor DEC205/CD205. Proc Natl Acad Sci u S A 2016;113:13438–43.
15. Faddaoui A, Bachvarova M, Plante M, Gregoire J, Renaud MC, Sebastianellim A, et al. The mannose receptor LY75 (DEC205/CD205) modulates cellular phenotype and metastatic potential of ovarian cancer cells. Oncotarget 2016;7:14125–42.
16. Giridhar PV, Funk HM, Gallo CA, Porollo A, Mercer CA, Plas DR, et al. Interleukin-6 receptor enhances early colonization of the murine omentum by upregulation of a mannose family receptor, LY75, in ovarian tumor cells. Clin Exp Metastasis 2011;28:887–97.
17. Kupchan SM, Komoda Y, Branfman AR, Sneden AT, Court WA, Thomas GJ, et al. The maytansinoids. Isolation, structural elucidation, and chemical interrelation of novel ansa macrolides. J Org Chem 1977;8:2349–57.
18. Kupchan SM, Komoda Y, Court WA, Thomas GJ, Smith RM, Karim A, et al. Maytansine, a novel antileukemic ansa macrolide from Maytenus ovatus. J Am Chem Soc 1972;94:1354–6.
19. Bouchard H, Viskov C, Garcia-Echeverria C. Antibody-drug conjugates- a new wave of cancer drugs. Bioorg Med Chem Lett 2014;24:5357–63.
20. Workman P, Aboagye EO, Balkwill F, Balmain A, Bruder G, Chaplin DJ, et al. Guidelines for the welfare and use of animals in cancer research. Br J Cancer 2010;102:1555–77.
21. Official Journal of the European Union. Directive 2010/63/Eu of the European Parliament and of The Council on the protection of animals used for scientific purposes of September 22, 2010. Available from: https://eur-lex.europa.eu/LexUriServ/LexUriServ.do?uri=OJ:L:2010:276:0033:0079:EN:PDF.
22. Gao H, Korn JM, Ferretti S, Monahan JE, Wang Y, Singh M, et al. High-throughput screening using patient-derived tumor xenografts to predict clinical trial drug response. Nat Med 2015;21:1318–28.
23. Mazot P, Cazes A, Dingli F, Degoutin J, Irinopoulou T, Boutterin MC, et al. Internalization and down-regulation of the ALK receptor in neuroblastoma cell lines upon monoclonal antibodies treatment. PLoS One 2012;7:e33581.
24. Perera RM, Zoncu R, Johns TG, Pypaert M, Lee FT, Mellman I, et al. Internalization, intracellular trafficking, and biodistribution of monoclonal antibody 806: a novel anti-epidermal growth factor receptor antibody. Neoplasia 2007;9:1099–110.
25. Terp MG, Olesen KA, Arnspang EC, Lund RR, Lagerholm BC, Ditzel HJ, et al. Anti-human CD73 monoclonal antibody inhibits metastasis formation in human breast cancer by inducing clustering and internalization of CD73 expressed on the surface of cancer cells. J Immunol 2013;191:4165–73.
26. Teicher BA. Anticancer drug development guide. Totowa, NJ: Humana Press; 1997.
27. Prigent C, Dimitrov S. Phosphorylation of serine 10 in histone H3, what for? J Cell Sci 2003;116:3677–85.
28. Leal M, Wentland J, Han X, Zhang Y, Rago B, Duriga N, et al. Preclinical development of anti-5T4 antibody-drug conjugate: pharmacokinetics in mice, rat, and NHP and tumor/tissue distribution in mice. Bioconjugate Chem 2015;26:2223–32.
29. Butter M, Morel AS, Jordan WJ, Eren E, Hue S, Shrimpton RE, et al. Altered expression and endocytic function of CD205 in human dendritic cells, and detection of a CD205-DCL-1 fusion protein upon dendritic cell maturation. Immunology 2007;120:362–71.
30. Ogitani Y, Hagihara K, Oitate M, Naito H, Agatsuma T. Bystander killing effect of Ds-8201a, a novel anti-human epidermal growth factor receptor 2 antibody–drug conjugate, in tumors with human epidermal growth factor receptor 2 heterogeneity. Cancer Sci 2016;107:1039–46.

Published OnlineFirst June 21, 2019; DOI: 10.1158/1535-7163.MCT-18-0624

Molecular Cancer Therapeutics

MEN1309/OBT076, a First-In-Class Antibody–Drug Conjugate Targeting CD205 in Solid Tumors

Giuseppe Merlino, Alessio Fiascarelli, Mario Bigioni, et al.

Mol Cancer Ther 2019;18:1533-1543. Published OnlineFirst June 21, 2019.